Numerical Modeling of Heat Transfer and Flow in Low Power Arcjet Thruster

Hai-Xing Wang[a, *], Shao-Xia Jia[a], Xi Chen[b], and Wenxia Pan[c]

[a] *Beijing University of Aeronautics and Astronautics, Beijing, 100191*
*(*corresponding author: whx@buaa.edu.cn)*
[b] *Tsinghua University, Beijing, 100084*
[c] *Institute of Mechanics, Chinese Academy of Sciences, Beijing, 100190*

Abstract. Modeling studies are preformed to investigate the plasma and heat transfer characteristics of a low power argon arcjet thruster. Computed temperature, velocity, static pressure, and Mach number distribution in arcjet thruster under typical operating condition are presented in this paper. It shows that the performance data from numerical modeling results are basically consistent with the experimental measured values

Keywords: Arcjet, Numerical Modeling, Heat Transfer, Fluid Flow
PACS: 52.80.Mg, 52.65.Kj, 47.27.Te

INTRODUCTION

An arcjet is an electrothermal propulsion device in which a gas propellant is heated by means of a high temperature arc. The propellant expands through a large area ratio nozzle to produce thrust. Due to high specific impulse and moderate thrust levels, arcjet thruster now are in use for north-south stationkeeping on commercial satellites. Despite the relative simplicity of the basic design, many complex physical processes are involved in arcjet thruster [1,2].

An understanding of the physical processes and design requirements of arcjet thruster is the key to advancing the technology. Although a lot of experimental and modeling results concerning the arcjet performance and characteristics have been accumulated in the literature, our understanding about complex physical processes in arcjet is still incomplete. The principle goal of this study is to understand the heat transfer and fluid flow processes within arcjet thruster and to provide preliminary estimates of the thruster performance. Our modeling is based on the full Navior-Stokes equations and thus viscous stress and dissipation terms are retained in the governing equations, the solution of which is based on the all-speed SIMPLE algorithm [3], which represents an extended form of the standard SIMPLE algorithm in order to be applicable to the present compressible flow case. From the computed temperature, velocity, static pressure, and Mach number contours, the features of subsonic-supersonic plasma flow and heat transfer within the arcjet can be identified.

MODELING APPROCAH

The main assumptions used in this study are as follows. (1) The plasma flow in the arcjet is steady, axi-symmetrical; (2) The plasma is optically thin and in LTE (local thermodynamic equilibrium) state; (3) The swirling velocity component can be neglected in comparison with the axial velocity; (4) Argon is considered as propellant. Figure 1 shows the computation domain used in this study, which includes fluid flow, cathode and anode region. The dimensions of this thruster are the same as used in the experimental investigations of Ref. [4]. Because of the axi-symmetry of flow in the arcjet thruster, only the upper half of the arcjet thruster is taken as the computational domain. Altogether 89 (z-direction)×30 (r-direction) grid points are employed in this study.

CP1233 *The 2nd International ISCM Symposium and The 12th International EPMESC Conference*
J. W. Z. Lu, A.Y.T. Leung, V. P. Iu, and K. M. Mok

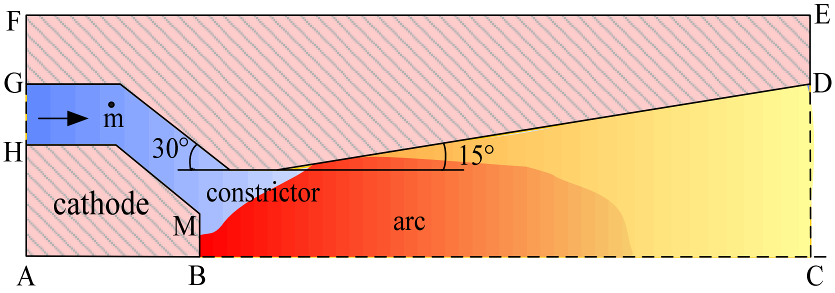

FIGURE 1. Schematic of arcjet thruster indicating fluid and anode domain

At the inlet section of the arcjet thruster, the stagnation pressure is fixed to be 2.5×105 Pa, the temperature being the room temperature, v=0, whereas the axial velocity component u is calculated from the isentropic stagnation property relations. The incoming gas flow rate is determined by the iteration process itself, as mentioned in Ref. [3]. Axi-symmetrical conditions are used at the arcjet axis, whereas the temperatures and velocities at the outlet section of the arcjet are calculated in the iteration process by extrapolating their values at the neighbor interior grid points to the outlet. At the surfaces of the anode nozzle and cathode, non-slip conditions are adopted. On the outer surface of arcjet thruster, the local heat flux is given by radiation to surroundings at specified background temperature and a constant emissivity of 0.31.

RESULTS AND DISCUSSION

Typical modeling results are shown in Figs. 2-9 for the present subsonic-supersonic of DC arcjet thruster with the arc current of 10 A and the inlet stagnant pressure of 2.5×10^5 Pa. The predict temperature distribution within the arcjet thruster is plotted in Fig. 2. It is seen the high plasma temperature appear in the downstream region of the cathode and near the arcjet axis, with the highest temperature of 14960 K. Along the arcjet axis, as shown in Fig. 3, the gas temperature at first increase very rapidly with increasing distance from the cathode tip until the highest temperature is achieved. It then decreases gradually as the plasma flow toward the arcjet exit.

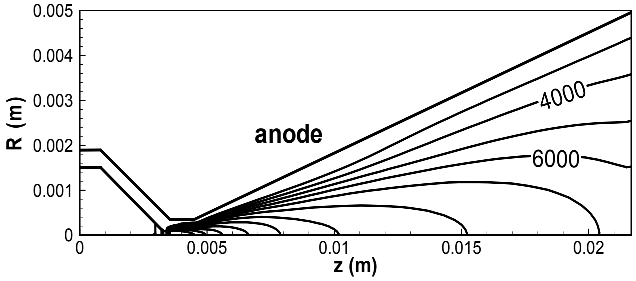

FIGURE 2. Computed temperature distribution within the arcjet (unit: 10^3 K, interval 1000 K)

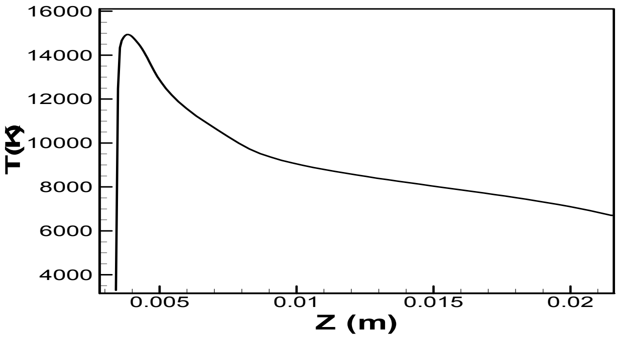

FIGURE 3. Computed temperature variation along the arcjet axis

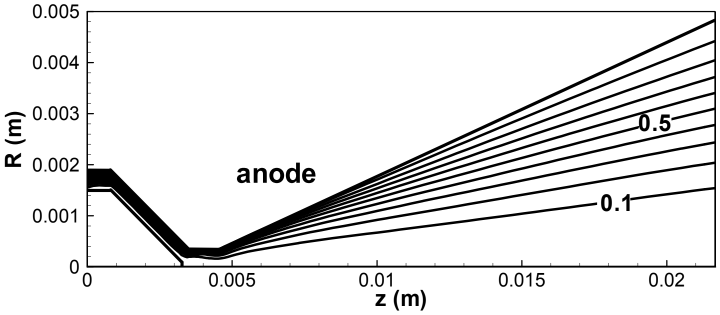

FIGURE 4. Computed streamlines within the arcjet (interval 0.1, corresponding to 6.3×10^{-5} kg/s)

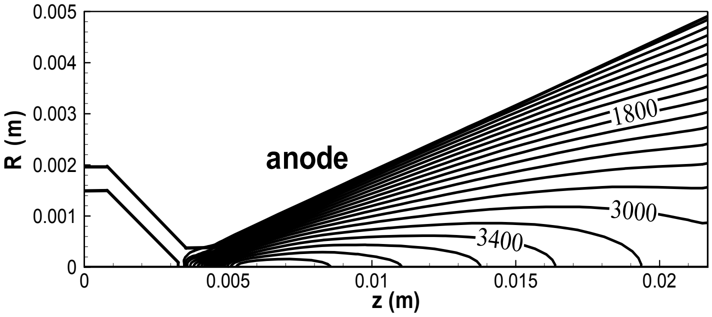

FIGURE 5. Computed axial velocity within the arcjet (unit: m/s, interval 200 m/s)

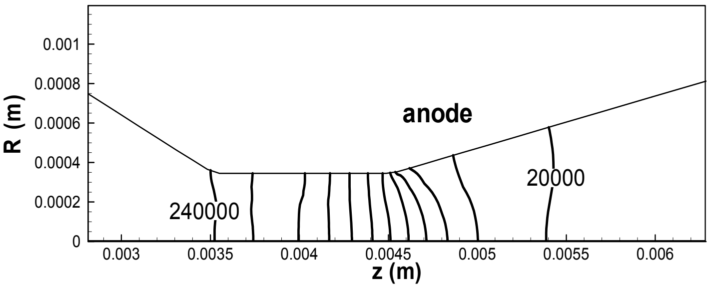

FIGURE 6. Computed static-pressure contours within the arcjet (units: Pa)

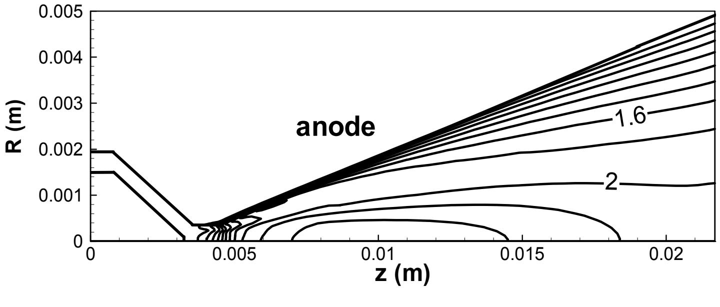

FIGURE 7. Computed Mach number contours within the arcjet (interal 0.2)

The predicted streamlines and axial velocity, static pressure, as well as Mach number contours, within the arcjet are shown in Figs. 4-7. The variation of ***u*** and ***p*** along the arcjet axis are further plotted in Fig. 8. Fig. 4 shows that most of the incoming argon mass flow rate concentrates in the region near the nozzle wall. From Figs. 6 and 8, it can be seen that static pressure decreases monotonously along the arcjet axis and is almost uniform at each cross section in the downstream region of the cathode, similar to the one-dimensional compressible flow in a nozzle. The axial velocity distribution along the arcjet axis is similar to the temperature variation along the arcjet axis, i.e. the axial velocity increase at first very rapidly and then decreases gradually as the plasma flows toward the arcjet exit.

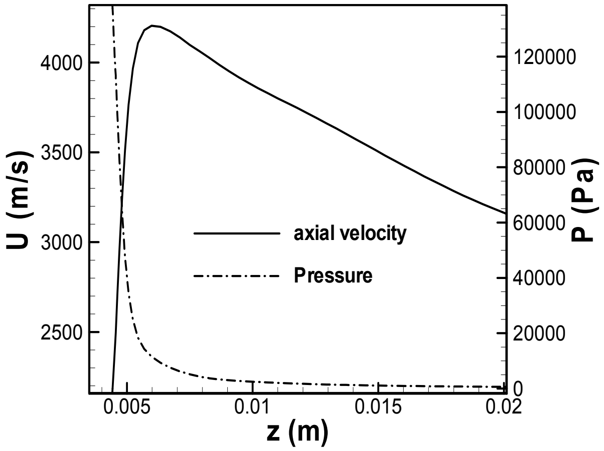

FIGURE 8. Computed axial velocity and static-pressure along the arcjet axis

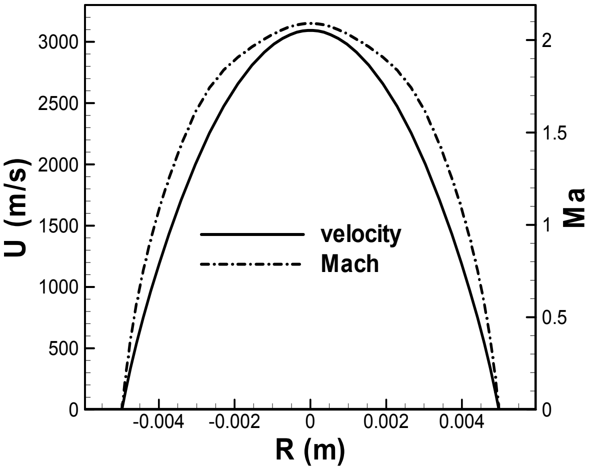

FIGURE 9. Computed axial velocity and Mach number profiles at the arcjet outlet section

A similar variation is also seen for the Mach number distributions in Fig. 7. From Fig. 7 it is concluded that the flow field can be approximately divided into three regions. Namely, within the convergent segment of the arcjet thruster, where plasma velocity is comparatively low, the flow is subsonic. Within the constritor of the arcjet, the plasma temperature begins to decrease while the velocity increases due to the energy transformation from the pressure energy into gas kinetic energy. The flow transits from subsonic to supersonic regime in the constrictor of arcjet. Within the divergent segment of the arcjet nozzle, the flow becomes completely supersonic. But at the downstream of arcjet nozzle, due to energy transfer between the arc and the cooler inner surface of arcjet nozzle, the axial velocity decrease from the maximum centerline velocity of 4205 m/s at an axial location z=5.5 mm to 3093 m/s at the exit plane. In Fig. 9, Mach number, axial velocity at the arcjet exit are given. A peak Mach number of Ma=2.1 is noted at the exit plane centerline.

As descirbed in previous section, the incoming gas mass flow rate can be determined from the simulation iteself. In the present modeling, the computed argon flow rate is 6.3×10^{-5} kg/s. Under these operating conditions, the computed specific impulse is 192 s. These performance data are basically consistent with the experimental measured values.

CONCLUSIONS

Modeling results are presented for the plasma flow and heat transfer characteristics in a low power argon arcjet thruster. Under the typical operating conditions for the case with the arc current is 10 A, the inlet stagnant pressure of 2.5×10^{5} Pa, the computed argon flow rate is 6.3×10^{-5} kg/s and the computed specific impulse is 192 s. These performance data are basically consistent with the experimental measured values.

ACKNOWLEDGMENTS

This work was supported by the National Natural Science Foundation of China (Nos. 50836007, 10621202).

REFERENCES

1. M. M. Sabchez, S. A. Miller. J. Propulsion and Power, Vol. 12 (6), pp. 1035-1043, (1996).
2. G. W. Butler, R. J. Cassady. J. Propulsion and Power, Vol. 12 (6), pp. 1026-1034, (1996).
3. P. Han and X. Chen, Plasma Chemistry and Plasma Processing, Vol. 21 (2), pp. 249–264, (2001).
4. H. J. Huang, W. X. Pan, X. Meng and C. K. Wu, Submitted to Chinese Physics Letter, (2009).